RESEARCH ARTICLE

Construction of a spatiotemporal graph neural network-driven decision support system for ecological safety management based on multisource pollution data

Peixuan Fu[1], Yali Zhang[2, *]

[1]Nanjing Police University, Nanjing, Jiangsu, China. [2]China Electronics Cloud Computing Co., Ltd., Nanjing, Jiangsu, China.

Received: May 27, 2025; **accepted:** October 8, 2025.

In modern environmental science, ecological safety is essential in eliminating pollution sources and complex interactions in dynamic environments. The existing methods fail to determine the relationship between the sources, which reduces risk assessment efficiency. This research applied spatio-temporal graph neural networks with decision support systems (ST-GNN and DSS) to maintain ecological safety. The ST-GNN approach utilized multisource pollution heterogeneous data including soil, air, and water. The fused information was frequently explored with the help of spatial and temporal components to identify the dependencies between the features that helped to predict ecological risk in various regions. In addition, the approach utilized data normalization and bi-directional modeling techniques to eliminate inconsistent and imputed values, thereby simplifying the analysis of risk scores. The fused data was processed using k-means clustering to group the regions, and the neural learning model was applied to categorize the areas into safety, risk, and alerts. The efficiency of proposed system was evaluated using the experimental results, in which the dependency analysis ensured 98% accuracy for air, 97.3% for water, and 97% for soil resources. The proposed system provided effective and actionable recommendations to ensure ecological safety and contributed to sustainable environmental management.

Keywords: ecology risk; water; air; soil resources; spatial dependencies; temporal analysis; graph neural networks; k-means clustering; decision support systems.

[*]**Corresponding author:** Yali Zhang, China Electronics Cloud Computing Co., Ltd., Nanjing, Jiangsu 210012, China. Email: zhangyali1998@hotmail.com.

Introduction

In today's world, human population activities are creating environmental degradation [1], especially soil, water, and air, which are highly affected by deforestation, industrial discharges, urbanization, waste management, and vehicular emissions [2]. The ecosystem is exposed to harmful chemicals including mercury, lead, nitrogen dioxide, particulate matter, chemical effluents, and carbon monoxide, which significantly impact agriculture, biodiversity, and endangered populations. Various traditional methods have been utilized to explore the relationship between spatial and temporal features to monitor and predict environmental traits and systems [3]. However, one of the main problems is the sheer variety of pollution data coming from different sources such as sensor networks, satellites, meteorological stations, and municipal data hubs [4]. The differences in time and the data heterogeneity create major

obstructions to integration and analysis. Conventional statistical techniques and elementary machine learning approaches do not cope well with such complex graph-like structures containing spatial dependencies like pollution diffusion across regions and temporal dependencies like seasonal pollution trend [5]. Many studies have tried to resolve these issues using a data-based approach, long short-term memory (LSTM) [6]. Deep learning models have been implemented for time-series forecasting of pollution level metrics [7], while random forests (RF) and support vector machines (SVMs) have been used for pollution classification [8]. However, these models also tend to overlook spatial correlations among data points, which is particularly problematic in ecological applications that are sensitive to where data is collected. Other recent work has focused on representing spatial relationships through specialized structures such as graph convolutional networks (GCNs) and GCN layers [9]. In the context of traffic or weather forecasting, temporal graph convolutional networks (T-GCNs) and spatiotemporal GCNs (ST-GCNs) have been created to incorporate spatial and temporal factors. For ecological purposes, the multi-faceted integration of diverse pollution data of air, water, and soil introduces complexities including noisy and missing sensor data streams and poses challenges in interpreting ecological risk levels [10, 11].

The most recent environment risk assessment process has integrated multisource data fusion and deep learning approaches to enhance the hierarchy of intelligence systems in predicting accuracy levels. Zhao *et al*. evaluated the ecological risk for the Harbin section of Songhua River Basin by applying multisource data hydrological merging and data integration algorithms of land use and water quality data. The results underscored the need for greater spatial precision concerning risk evaluation through dataset amalgamation based on multi-dimensional datasets [12]. However, the approaches were limited to water systems and did not incorporate soil and air pollution monitoring or other temporal variations. Zhang *et al*. developed a deep learning model (DLM) for anticipating the quality of treated effluents from wastewater treatment facilities and found that the model achieved high accuracy in outflow forecasting using operational and chemical sensor data streams [13]. Although this research exemplified the application of deep learning for mitigating environmental compliance burden, it was limited to considering water pollution and did not examine other multi-ecosystem spatial interactions or systems dynamics. Cai *et al*. advanced a novel computation-based solution to address challenges related to air pollution by developing an air quality monitoring system through the introduction of a system-integrated edge and cloud computing with the internet of things (IoT) data and deep learning modules to provide real-time, low-power air quality information at different locations [14]. While proving robust energy efficiency and scalability, their model demonstrated limitations with a simplistic approach attuned solely to atmospheric data without incorporating crucial soil or water parameters for holistic ecological evaluation. Jiang *et al*. trained a deep learning model on industrial discharge and environmental data to predict the concentration levels of heavy metals in urban sewer networks [15]. The study highlighted a neural network's ability to pinpoint spatial hotspots across sewage cleaning systems. Wang *et al*. presented a multifusion deep learning model (MF-DL) that applied satellite imagery, meteorological data, and ground sensor information for fire detection with a high degree of reliability, demonstrating the merit of multi-modal fusion for safety system frameworks [16]. However, this model was designed for detecting acute changes rather than ongoing observation, which made it inappropriate for long-term pollution surveillance and ecological change pattern recognition over time. Chen *et al*. proposed a deep learning model of citywide air quality prediction that estimated air quality by assimilating data from traffic, weather, and satellite information. The model maintained adequate air quality forecasting and mapping for public notification and decision-making for

policymaking concerns [17]. However, the model did not address cross-medium fusion, ecological risk assessment, or multi-domain analysis, which limited its practicality for air pollution. Zhang *et al.* developed a hybrid artificial intelligence model (HAIM) for the river ecosystem domain by combining numerous physical, chemical, and biological parameters to assess the river health for the Qinghai-Tibetan Plateau [18]. While the model provided a comprehensive understanding of river ecosystems, the scope of the model was static and geographically bounded and did not consider dynamic spatiotemporal changes over time and the interactions with atmospheric or terrestrial data. Further, Wang *et al*. created an advanced monitoring system of marine pollution using deep learning algorithms to foster carbon neutrality by integrating satellite data, marine sensors, and climate indicators to track pollutants in ocean ecosystems [19]. The model's insightful features and deep focus on ocean geography made it less useful for holistic ecological protection management for land and marine systems.

Many studies and the current available models have focused on monitoring the environment, emphasizing the importance of deep learning and multisource data fusion. However, there is an evident lack of merging datasets that pertain to air, water, and soil pollution into one model that is sensitive to time and offers ecosystem-centric intelligence. Further the current studies do not consider a decision support system (DSS) framework that would assist an environmental scientist or policy analyst in making sense of the results. There is an alarming gap in models that not only estimate pollution levels but also provide insights into identifying high-risk ecological zones, implementing advanced warning systems, and offering active foresight suggestions. This research proposed a novel decision support system based on a spatiotemporal graph neural network (ST-GNN). The system comprised a holistic ecological security graph structure that integrated pollution data from multiple sources to overcome these current challenges by combining a deep learning model with a graphical representation of spatial relationships, a dynamic prediction unit for capturing temporal trends, and a multimodal integrator for combining different pollution inputs. The proposed model incorporated fusion, forecasting, and powering ecological intelligence systems designed to support decision-making involving risk assessment, region classification, and policy suggestion.

Materials and methods

Construction of ST-GNN system with the DSS framework

The ST-GNN with DSS approach utilized multisource data fusion, spatial relationship analysis, and temporal learning to provide an intelligent, scalable, and robust framework for ensuring ecological safety in a changing environment. The gathered information was explored using the graph-based deep learning model that examined the spatial relationship and temporal dependencies between the features used to make effective decision support systems while managing ecological safety. The proposed system was designed to adapt to real-time data to ensure stakeholders' effective interpretation. The system integrated all components of the ST-GNN with DSS including air, water, and soil sensors as data sources, which captured data and sent to a central unit. The retrieved data was then preprocessed and fused to form a spatiotemporal collection before sending to the ST-GNN module for data partitions into space and time portions over graphs, allowing for tracking changes and capturing sequential events using recurrent units. The data retrieved from the model was sent to the decision support engine, allowing the user to view risk zones, estimate pollution diffusion, and provide other associated strategic advice (Figure 1).

Data collection

This study utilized three datasets including air, water, and soil information to identify the specific region's risk. The urban air pollution dataset was employed for air quality data

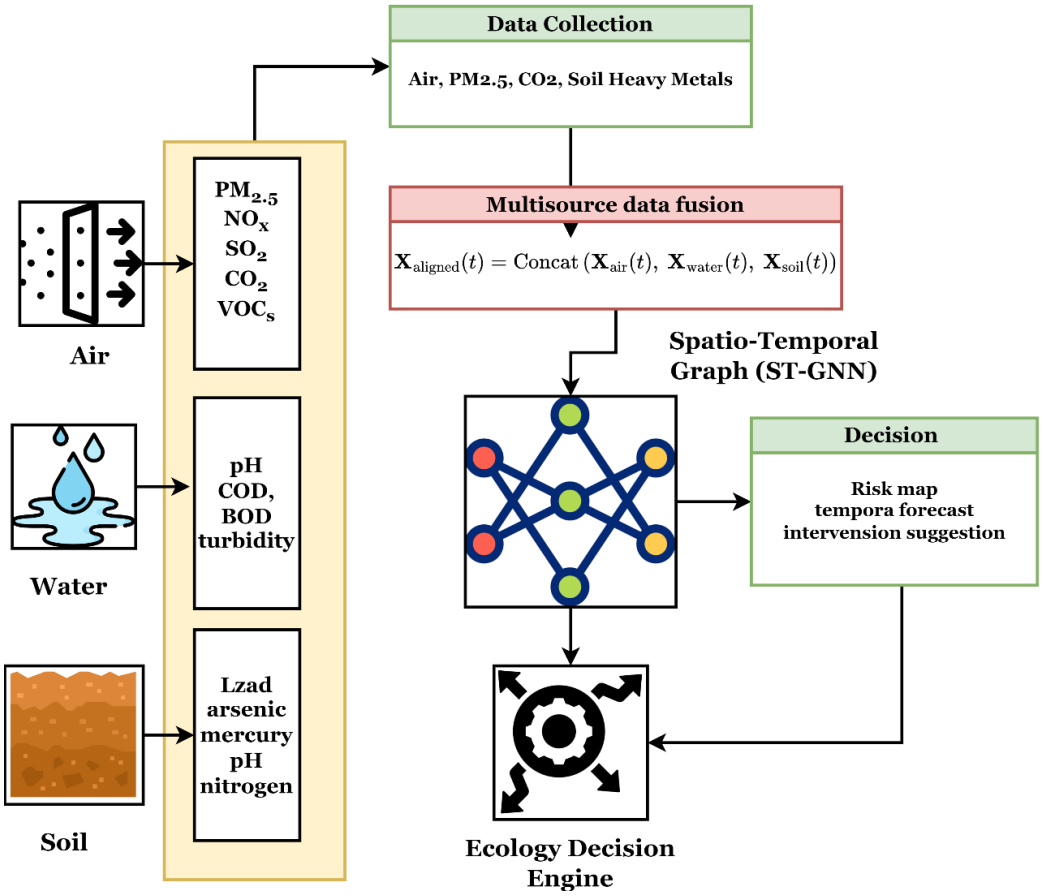

Figure 1. Overall structure of ST-GNN-based ecology risk management.

(http://kaggle.com/datasets/alfredkondoro/urban-air-pollution), which contained multiple features including satellite information, meteorological data, and other relevant factors for predicting ground-based measurements of PM2.5 in 10 cities. The river water quality prediction dataset (https://www.kaggle.com/code/vbmokin/datasets-for-river-water-quality-prediction) was used for water quality evaluation, which comprised data from eight successive stations of a water monitoring system located in 6 cities. The soil pollution and associated health impacts (https://www.kaggle.com/datasets/khushikyad001/soil-pollution-and-associated-health-impacts) was used for soil pollution data, which covered 14 cities with the data volume depending on the local intensity of land use. Totally, the research covered 14 cities in five provinces of China, among which 18,450 records from Metroville, Eastport, and Rivertown were retrieved from the eastern provinces, while 15,320 records were from the northern provinces including Northvale, Hillcrest, and Lakeford. Southgate and Brookfield made up the Southern provinces with 12,780 records, while the Capital City, Greenfield, Westford, and Plainview formed the central provinces with 20,560 records. Western provinces were composed of Westhaven and Stonebridge with 10,890 records. The system considered the volume of PM2.5, nitrogen oxides (NOx), sulfur compounds (SO_2), carbon compounds (CO_2), and volatile organic compounds (VOCs) as the constituents of air pollution. The pH value, concentration of heavy metals, chemical oxygen demand (COD), and biological oxygen demand (BOD) were applied as parameters to assess water quality. The data on

toxic elements such as lead (Pb), arsenic (As), mercury (Hg), and soil nutrients like soil pH and nitrogen content were used to monitor soil pollution. The system adopted spatiotemporal granularity as the data collection framework and geo-tagged the data points using global positioning system (GPS).

Multisource data fusion

A multisource data fusion engine was used to transform rich data resources into one cohesive spatiotemporal framework for deep learning applications, which included data cleaning through normalization and anomaly detection, time alignment, fusion, and imputation, and usable outputs preparation from input data streams (Figure 2). The parameters of the gathered sources varied in scale, unit, and range, which required the normalization process to scale the features in the range of $[0, 1]$ and were defined below.

$$\left.\begin{aligned} X_{i,j}^{norm} &= \frac{X_{i,j} - \min(X_i)}{\max(X_i) - \min(X_i)} \\ X_{i,j} &= \min(X_i), X_i = 0 (normalized value) \\ X_{i,j} &= \max(X_i), X_i = 1\ (normalized\ value) \end{aligned}\right\} \quad (1)$$

where X_i was the input value that was continuously explored to identify the minimum $\min(X_i)$ and maximum $\max(X_i)$ values for identifying the $X_{i,j}^{norm}$. The normalized data were resampled (daily or hourly) and synchronized to the general timeline $t \in T$. For every t, the fusion matrix $X_{aligned}(t)$ was developed by combining the $X_{i,j}^{norm}$ from every source as follows.

$$\begin{aligned} X_{\text{aligned}}(t) &= \text{Concat}(X_{\text{air}}(t),\ X_{\text{water}}(t),\ X_{\text{soil}}(t)) \\ X_{\text{air}}(t) &\in \mathbb{R}^{N\times F_{\text{air}}}, X_{\text{water}}(t) \in \mathbb{R}^{N\times F_{\text{water}}}, X_{\text{soil}}(t) \in \mathbb{R}^{N\times F_{\text{soil}}} \\ \Rightarrow X_{\text{aligned}}(t) &\in \mathbb{R}^{N\times(F_{\text{air}}+F_{\text{water}}+F_{\text{soil}})} = \mathbb{R}^{N\times F} \end{aligned} \quad (2)$$

where t was the time step. N was the number of sampling locations. $F_{\text{air}}, F_{\text{water}}, F_{\text{soil}}$ were the number of pollutant parameters. The total number of fused features was represented as $F = F_{\text{air}} + F_{\text{water}} + F_{\text{soil}}$. Concat$(\cdot)$ was the concatenation operation of fused features. $X_{\text{aligned}}(t)$ was the completely fused feature matrix. After fusing the features, the missing data imputation actions were required by applying bidirectional gated recurrent units, which helped predict missing values by exploring both future and past temporal context. The imputations were calculated in every state of the gated recurrent networks as follows.

$$\left.\begin{aligned} \vec{h}_t &= \text{GRU}_{fwd}\left(X_{aligned}(t-1), \vec{h}_{t-1}\right) \\ \overleftarrow{h}_t &= \text{GRU}_{bwd}\left(X_{aligned}(t+1), \overleftarrow{h}_{t+1}\right) \\ \hat{X}_{aligned}(t) &= \sigma(W[\vec{h}_t \parallel \overleftarrow{h}_t] + b) \end{aligned}\right\} \quad (3)$$

where $\vec{h}_t, \overleftarrow{h}_t$ were forward and backward hidden states. $\parallel$ was concatenations. W, b, and $\sigma(\cdot)$ were learnable parameters, which was represented as the sigmoid activation function. According to the computed $\hat{X}_{aligned}(t)$ values, the bi-directional smoothing process replaced the missing values with high-temporal coherence values, which helped management of the environmental trends effectively. The adaptive thresholding method was then applied to predict the outliers in the data. The outliers were detected with the help of z-score points that were computed as below.

$$\begin{cases} z_{i,j}(t) & = \frac{X_{\text{aligned}}^{i,j}(t) - \mu_{i,j}}{\sigma_{i,j}} \\ \text{where}\mu_{i,j} & = \frac{1}{T}\sum_{t=1}^{T} X_{\text{aligned}}^{i,j}(t), \\ \sigma_{i,j} & = \sqrt{\frac{1}{T}\sum_{t=1}^{T}\left(X_{\text{aligned}}^{i,j}(t) - \mu_{i,j}\right)^2} \end{cases} \quad (4)$$

where $X_{\text{aligned}}^{i,j}(t)$ was the raw input features with t alignment for i and j locations. $\mu_{i,j}$ was the mean feature of j[th] location. $\sigma_{i,j}$ was the standard deviation. $z_{i,j}(t)$ were standardized feature values. $|\ z\ | > 3$ was set as the threshold value. If this condition was satisfied, the input feature was considered an outlier, and its values were replaced using non-anomalous timestamps. After eliminating the irrelevant information and outliers from the dataset, the spatiotemporal graph was constructed to analyze the relationship between the features, which helped to predict ecological risk.

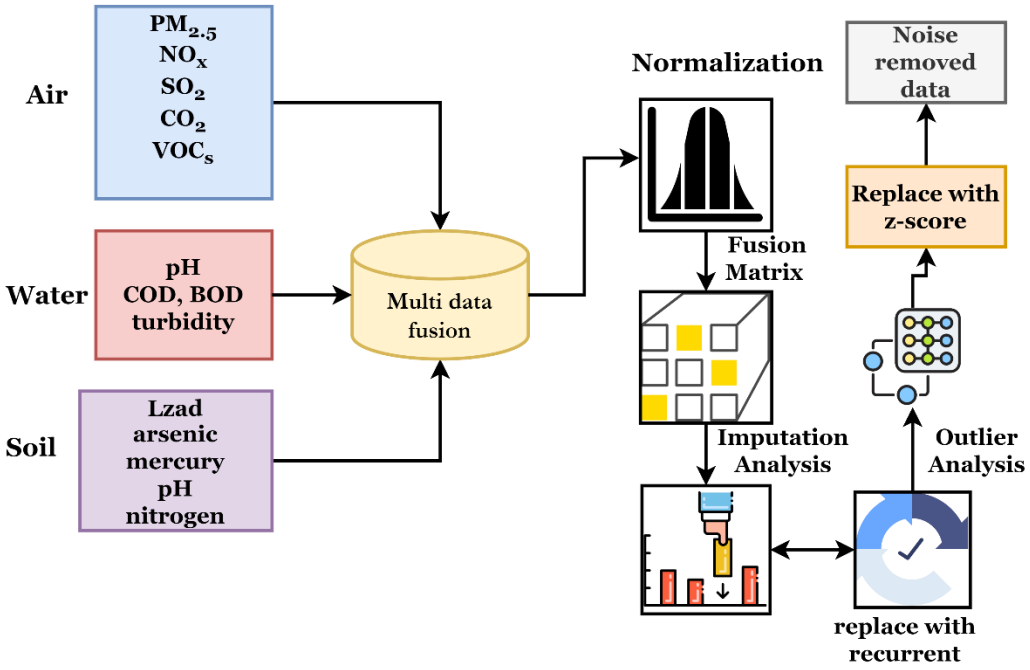

Figure 2. Multisource data analysis.

Construction of Spatiotemporal graph

The dynamic spatiotemporal graph $G(V, E)$ was constructed to represent the dependencies of diverse ecological sites over a period. Each node $v_i \in V$ in the graph represented a unique geo-tagged ecological observation site, which might include river basin checkpoints, air monitoring towers, or soil sensor locations. The edges E captured spatial and pollution-based proximity relations among these locations. The spatial adjacency matrix was first generated by computing the spatial proximity between the $i\ and\ j$ locations, which were modeled with the help of geographical distance $A_s(i,j) = \exp\left(-\frac{\text{dist}(i,j)^2}{\sigma^2}\right)$. The Euclidean distance was defined as $\text{dist}(i,j)$, and the scaling parameter was σ. The pollution correlation matrix was then formed by computing the pollution correlation between the locations, which was estimated using the multivariate pollution time series $A_p(i,j) = \text{corr}(X_i, X_j)$. Aligned pollution features were time series vectors X_i, X_j. Pearson correlation coefficients $\text{corr}(\cdot)$ were utilized. The estimated correlation $(corr(\cdot))$ was used to identify pollution trends in two distant zones. The extracted features and spatial relationships were fused by constructing the hybrid adjacency matrix $A_{\text{hybrid}} = \alpha A_s + (1-\alpha)A_p$, where A_s was distance-based adjacency, A_p was pollution similarity, and $\alpha \in [0,1]$ was tunable hyperparameters. The α parameters were adjusted to prioritize the spatial and similarity structures to predict pollutant dispersion and pollution hotspots. The dynamic temporals were extended with the help of the $G_t(V_t, E_t)$ at time step t. The time index graph sequence was fed as the input to the networks $\{G_1, G_2, \ldots, G_T\}$ that shared the common node but differed in edge weights because of the pollution correlations. In addition, the pollutants' spatial diffusions and temporal evolution patterns were estimated by combining the subsequent learning (temporal encoders and convolution operations) to predict the changing ecological landscapes. The structure of the ST-GNN block was shown in Figure 3. The critical component of ST-GNN was the spatial component, which controlled graph convolution neural networks that derived the spatial dependencies between the nodes in the ecology. The nodes were related to the distinct water, air, and soil sensor locations. Every $v_i \in V$

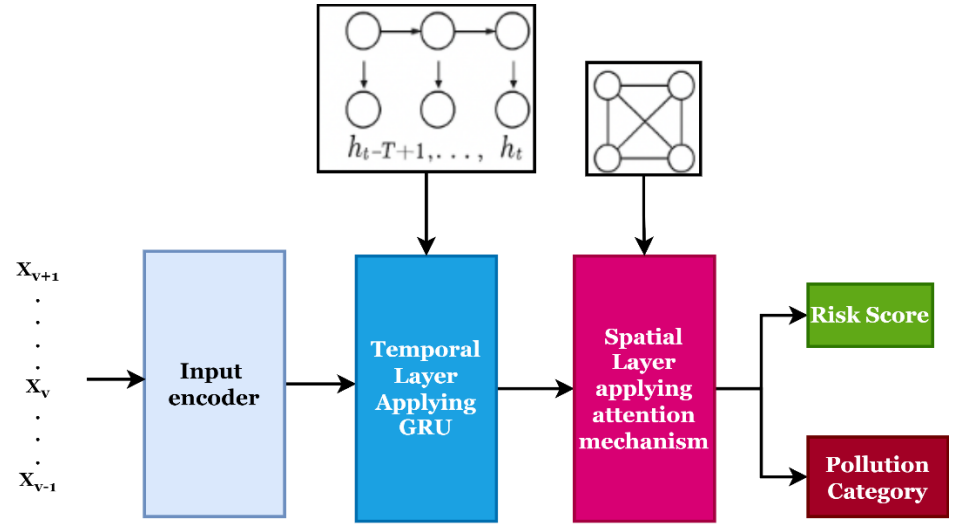

Figure 3. Flow chart of proposed spatiotemporal graph neural network.

node had features $X_i(t) \in \mathbb{R}^F$ at time t. From the computed $A_{\text{hybrid}} \in \mathbb{R}^{N\times N}$, the spatial graph convolution operation for l was calculated as below.

$$\left.\begin{aligned} H^{(l+1)} &= \sigma\left(\tilde{D}^{-1/2}\tilde{A}_{\text{hybrid}}\tilde{D}^{-1/2}H^{(l)}W^{(l)}\right) \\ \tilde{A}_{\text{hybrid}} &= A_{\text{hybrid}} + I \\ \tilde{D}_{ii} &= \sum_j \tilde{A}_{\text{hybrid},ij} \\ \hat{A} &= \tilde{D}^{-1/2}\tilde{A}_{\text{hybrid}}\tilde{D}^{-1/2} \\ Z^{(l)} &= \hat{A}H^{(l)}W^{(l)} \\ H^{(l+1)} &= \sigma(Z^{(l)}) = \sigma\left(\hat{A}H^{(l)}W^{(l)}\right) \end{aligned}\right\} \quad (5)$$

where $\tilde{A}_{\text{hybrid}} = A_{\text{hybrid}} + I$ was augmented adjacency, which was normalized $\hat{A}$ and propagated $Z^{(l)}$. The activation function was applied $\sigma(Z^{(l)})$ to get the output value. The degree matrix ($\tilde{D}$) was used to estimate the $\tilde{A}_{\text{hybrid}}$. $W^{(l)}$ was defined as trainable weight parameters. According to the spatial relationship, the pollution propagation patterns with neighboring dependencies were captured successfully. Once the spatial features were extracted, attention mechanisms captured trends that changed over time. The model executed multi-head attention on the temporal aspect of the node features. For every $H_i = [h_i(t-T),\ldots,h_i(t)] \in \mathbb{R}^{T\times d}$ sequence embedding, self-attention was framed as follows.

$$\left.\begin{aligned} \text{Attention}(Q,K,V) &= \text{softmax}\left(\frac{QK^T}{\sqrt{d_k}}\right)V \\ \tilde{H}_t &= \text{Softmax}\left(\frac{(H_tW_Q)(H_tW_K)^{\top}}{\sqrt{d_k}}\right)(H_tW_V) + H_t \end{aligned}\right\} \quad (6)$$

where the attention mechanism was computed for the number of nodes (N) $(ecology\ sites)$, feature channel (F), and temporal window (T). $W_Q, W_K, W_V \in \mathbb{R}^{F\times d_k}$ learnable weight matrix was estimated for key, query, and value transformation. $\sqrt{d_k}$ scaling vector was applied to manage the stability, and $(H_tW_Q)(H_tW_K)^{\top}$ was used to perform the similarity comparison. The computed $\tilde{H}_t \in \mathbb{R}^{N\times F\times T}$ was fed into the ST-GNN layer, which effectively identified the highly polluted areas. The attention mechanism gave the risk score (0 to 1) using the $\hat{y}_v^t = \sigma(W_o\mathbf{z}_v^t + b)$, in which the pollutions were categorized as low, medium, and high by applying the softmax function. Let X_s be the spatial features that were obtained from the spatial component, X_t was the temporal features derived from the attention mechanism, the fused $X_{fused} = \text{Fusion}(X_s, X_t)$ was used to identify the spatial dependencies and temporal dynamics. During the fusion, the weighted sum values $X_{fused} = \alpha X_s + \beta X_t$ was

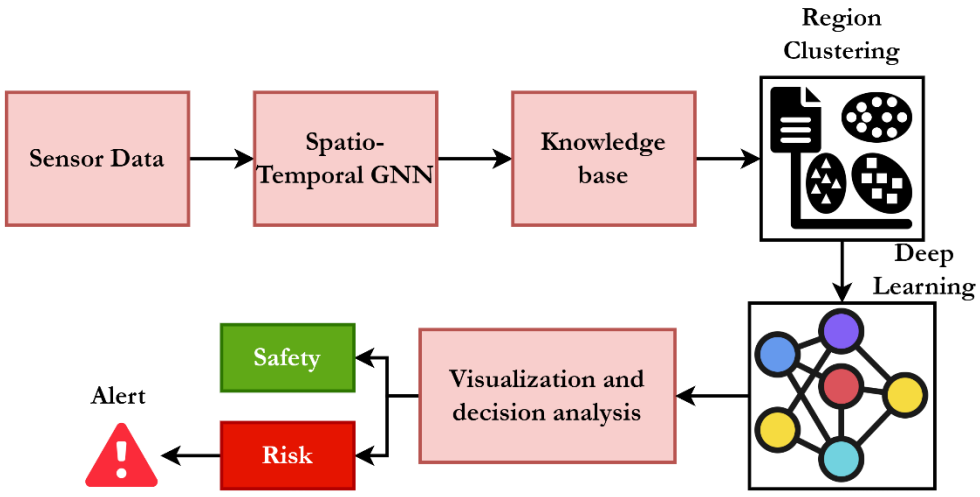

Figure 4. Process flow of decision support on ecological risk management.

used to get the feature importances. After identifying the feature dependencies and fused features, they were fed into the decision support systems to determine the risk factors to create ecological safety management.

Ecology decision engine

The environmental decision engine integrated input models' outputs into a comprehensive decision support dashboard for ecological risk monitoring and management, which featured ecological real-time tracking and active risk management and included ecological risk maps, temporal forecasts, and intervention suggestions. The ecological risk maps utilized spatiotemporal risk score information and heatmap creation techniques to display geographic areas of interest on the map, highlighting different levels of risk, which aided stakeholders in locating and taking swift action on zones with the highest observed risk. Temporal forecasts took advantage of the learned temporal attention mechanisms to estimate what would happen in the future, in terms of the spread and concentration of pollutants or environmental hazards, enabling strategic foresight in planning. The intervention suggestions translated model output into alerts, adaptive thresholds, and actions recommended to mitigate those risks. The unsupervised K-means method divided the set of zones into dynamically defined ecological units based on pattern changes in pollution over time. These clusters were then attached to classification models of neural networks, which allocated each region into previously defined zones of environmental safety as safe, alert, and critical. The classification changed with ongoing learning from the data's historical trends, seasonality, and feedback from the environment, ensuring that boundaries were context-sensitive and responsive. The decision engine interpreted complicated information while maintaining the geometric integrity of the strategies and policies in place, which captured the essence of proactive prevention in maintaining robust eco-safety and enabled tailored prompt action (Figure 4). The fused features were fed into the k-means clustering process to perform the zone segmentation and neural network classification to categorize the risk. Let $X_{fused} = \{x_1, x_2, \ldots, x_n\}$ be the fused features in various spatial regions, the clustering process divided the data into K clusters to minimize the within-cluster sum of squares, which were represented as $\min_C \sum_{k=1}^{K} \sum_{x_i \in C_k} \| x_i - \mu_k \|^2$. The set of clusters was denoted as C_k and the cluster centroid was represented as μ_k. This process helped identify the ecological zones categorized

according to the spatiotemporal context, variations, and pollution intensity. The feedforward network then analyzed the inputs, categorizing them as safe, alert, or critical. The point x_i was fed into the network that predicted the output as follows.

$$\left.\begin{aligned} h^{(1)} &= \sigma\left(W^{(1)}x_i + b^{(1)}\right) \\ h^{(2)} &= \sigma\left(W^{(2)}h^{(1)} + b^{(2)}\right) \\ h^{(2)} &= \sigma(W^{(2)}h^{(1)} + b^{(2)}) \end{aligned}\right\} \quad (7)$$

where the non-linear activation function was $\sigma(\cdot)$. The weights and bias value were denoted as $W^{(i)}\ and\ b^{(i)}$. The probability distribution of the three classes was represented as $\hat{y} \in \mathbb{R}^3$. During the output estimation, the model was trained with the help of the cross-entropy loss $\mathcal{L} = -\sum_{j=1}^{3} y_j \log(\hat{y}_j)$ to minimize the output deviations, where y_j was the true label for j, and the predicted probability was $\hat{y}_j$. Then the total loss was computed as follows.

$$\left.\begin{aligned} \mathcal{L} &= \lambda_1 \cdot \mathcal{L}_{cls} + \lambda_2 \cdot \mathcal{L}_{reg} + \lambda_3 \cdot \mathcal{L}_{smooth} \\ \mathcal{L}_{reg} &= \frac{1}{N}\sum_i \| R_i^t - R_i^{t-1} \|_2^2 \\ \mathcal{L}_{smooth} &= \frac{1}{|E|}\sum_{(i,j)\in E} \| R_i^t - R_j^t \|_2^2 \end{aligned}\right\} \quad (8)$$

The results produced by the neural networks were displayed using a decision support dashboard that depicted ecological risk maps, temporal forecasts, and intervention suggestions. Limits for alerts were incrementally adjusted from historical trends and turned over time, allowing the system to adapt to ecological decision-making regarding safety.

Efficiency evaluation of proposed system

The efficiency of the proposed system was evaluated and compared with existing methods including deep learning model (DLM) [13], multi-modal fusion with deep learning model (MF-DL) [16], and hybrid artificial intelligence model (HAIM) [18].

Results and discussion

Data size-based efficiency analysis

The results showed that the proposed ST-GNN model had perpetually surpassed the baseline models of DLM, MF-DL, and HAIM including data size and all tracked performance metrics. With a data size of 1,000, ST-GNN surpassed all other models in mean absolute error (MAE) (0.076) and root mean square error (RMSE) (0.119), while also surpassing others in R^2 (0.974) and F1-score (0.98), which portrayed commendable predictive accuracy and classification prowess. Moreover, ST-GNN spent the least computation time (8.6s), making it the most efficient one (Table 1). This model outperformed others by incorporating spatiotemporal dependencies through graph convolution and temporal attention. Further, the model could capture dynamic pollution patterns more efficiently with this capability. With ST-GNN, the hybrid graph structure and attention mechanisms enabled it to extract richer, context-aware features to make accurate and more stable predictions in complex multisource environmental data.

Data source-based efficiency analysis

The system's efficiency was also evaluated for different data sources. The results demonstrated that the proposed system showed outstanding performance compared to other models. In every situation, ST-GNN showed the lowest MAE and RMSE, demonstrating prediction accuracy and better performance. Furthermore, the proposed system achieved the best R^2 and F1 scores, demonstrating the accuracy and reliability of regression and classification. The results showed that MAE in air quality predictions from ST-GNN was 0.094, while R^2 was 0.98 and F1 score was 0.974, and all attained at an efficient computation time of 3.9 s, surpassing the other compared models. Water and soil datasets also exhibited similar trends with ST-GNN's R^2 consistently above 0.97 and F1 scores around 0.98 (Table 2). The system's spatiotemporal graph structure approximated the spatial correlation between location and temporal dynamics. Furthermore, ST-GNN captured

Table 1. Data size-based efficiency analysis of the ST-GNN ecology risk management system.

Data size	Model	MAE	RMSE	R^2	F1-score	Computation time (s)
10	DLM	0.182	0.261	0.81	0.872	2.4
	MF-DL	0.161	0.238	0.85	0.897	3.1
	HAIM	0.145	0.217	0.958	0.927	3.8
	ST-GNN	0.122	0.194	0.972	0.985	2.0
100	DLM	0.149	0.212	0.88	0.78	3.9
	MF-DL	0.137	0.201	0.921	0.82	4.2
	HAIM	0.128	0.187	0.963	0.86	4.9
	ST-GNN	0.104	0.159	0.98	0.971	2.9
500	DLM	0.124	0.184	0.82	0.82	6.7
	MF-DL	0.113	0.169	0.85	0.85	6.9
	HAIM	0.106	0.154	0.937	0.878	7.1
	ST-GNN	0.085	0.131	0.982	0.965	5.5
1000	DLM	0.118	0.172	0.84	0.85	11.0
	MF-DL	0.107	0.159	0.86	0.88	11.3
	HAIM	0.099	0.146	0.89	0.931	11.7
	ST-GNN	0.076	0.119	0.974	0.98	8.6

Table 2. Data source-based efficiency analysis of the ST-GNN ecology risk management system.

Data source	Model	MAE	RMSE	R^2	F1-score	Computation time (s)
Air	DLM	0.143	0.211	0.89	0.81	4.6
	MF-DL	0.131	0.198	0.92	0.85	4.8
	HAIM	0.118	0.181	0.95	0.928	5.1
	ST-GNN	0.094	0.145	0.98	0.974	3.9
Water	DLM	0.137	0.202	0.8	0.79	4.4
	MF-DL	0.124	0.188	0.93	0.84	4.6
	HAIM	0.115	0.171	0.96	0.937	5.0
	ST-GNN	0.089	0.141	0.973	0.98	3.6
Soil	DLM	0.139	0.204	0.77	0.78	4.8
	MF-DL	0.127	0.19	0.85	0.83	5.1
	HAIM	0.113	0.176	0.88	0.936	5.5
	ST-GNN	0.088	0.138	0.97	0.97	4.1

complex dependencies between pollution type and location that were not exploited by other models.

Efficiency analysis

Leveraging the attention mechanism gave far more accurate and dependable results. The system's efficiency was evaluated using precision, recall, accuracy, and mean square error rate (MSE). The results showed that the proposed ST-GNN consistently outperformed the competitors in all evaluation and data source measures. In terms of air, water, and soil datasets, ST-GNN achieved 0.98, 0.973, and 0.97 accuracies, respectively, sharply outperforming HAIM, MF-DL, and DLM models. This performance was further confirmed by the comparison of precision and recall, where the ST-GNN scored the highest rank among the others with low false positive and false negative counts. In addition, ST-GNN reached the highest marks in regression tasks measured by the MSE, which commended its stability in prediction-focused tasks (Figure 5). The proposed model's

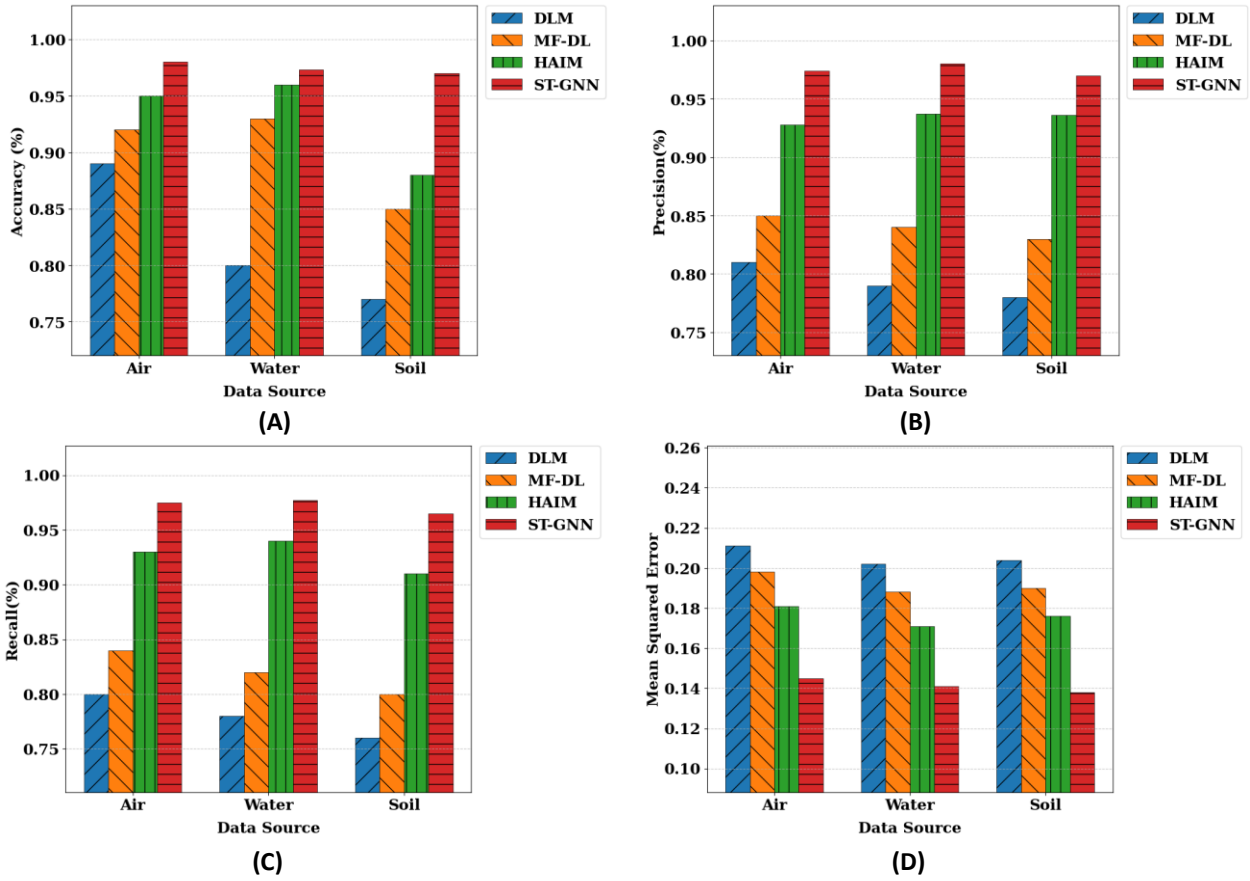

Figure 5. Efficiency analysis of ST-GNN-based ecology risk exploration. **A.** accuracy. **B.** Precision. **C.** Recall. **D.** MSE.

performance stemmed from its unique architecture that captured spatial and temporal dependencies found in environmental data. ST-GNN did not take the conventional routes of treating spatial and temporal features separately or oversimplifying to linear rules. Instead, it used the attention mechanisms to focus on critical temporal patterns. Attention-based engines enabled ST-GNN to drastically decrease the overhead of identifying dynamic systems by focusing on the events themselves in real time alongside trends. The model's capability to sustain superior performance across different environmental media of air, water, and soil further illustrated its general acuity, underscoring its usefulness for multi-faceted ecological monitoring systems where cross-media data characteristics varied spatially and hierarchically. From this perspective, the proposed ST-GNN marked a significant leap forward in modeling environmental data due to its increased accuracy in making predictions that could improve management decisions concerning pollution and ecological degradation. This proposed method successfully explored the relationship between the features that predicted the environmental risk by exploring the essential data sources compared to the other methods.

Conclusion

This research developed an ecological monitoring system that predicted ecological risks by integrating multisource pollution data and utilizing a decision support model enhanced by a spatiotemporal graph neural network (ST-GNN). The model applied data normalization and bi-directional modeling techniques to eliminate irrelevant information before fusing multi-modal

data to identify the spatial and temporal relationship between the features. From the fused information, the attention mechanism was applied to identify the risk score to classify the ecological regions with maximum accuracy, which enabled greater prediction and management of ecological risks. However, the system faced several drawbacks including its reliance on an adequate and optimal dataset. Operational capabilities would be suboptimal in less polluted regions or zones with sparse information due to the system's intricate layered data structure, real-time deployment on large geospatial datasets, limited system resources, and financial constraints. Future work should focus on how to provide optimal performance in data-sparse regions while enhancing the generality, accuracy, and adaptability of the system. Furthermore, redefining the model structure to adapt to real-time conditions and incorporating additional environmental variables would improve the prediction and application capabilities of the system and help enhance the ecological monitoring system.

Acknowledgements

This work was supported by Basic Research Funds for Central Universities “Study on the Co-governance Mechanism of Ecological Police from the Perspective of County Governance” (Grant No. RWZD202503）.

References

1. Vass H, Mănescu C, Sicoe-Murg O, Mateoc T, Mateoc-Sîrb N. 2021. Study on climate change issue and environmental degradation in Romania. Agric Manag/Lucr Stiint Ser I Manag Agricol. 23(2):89-96.
2. Saxena V. 2025. Water quality, air pollution, and climate change: Investigating the environmental impacts of industrialization and urbanization. Water Air Soil Pollut. 236(2):1-40.
3. Hoque SR, Sultana SR. 2024. Addressing global environmental problems: Challenges, solutions, and opportunities. Soc Sci Rev Multidiscip J. 2(2):124-130.
4. Haider H, Lavanya B. 2024. Revolutionizing Agritech with deep learning-enhanced remote sensing for precision agricultural management. PatternIQ Mining. 1(3):63-76.
5. Ang KLM, Seng JKP, Ngharamike E, Ijemaru GK. 2022. Emerging technologies for smart cities' transportation: Geo-information, data analytics and machine learning approaches. ISPRS Int J Geo-Inf. 11(2):85.
6. Barthwal A, Goel AK. 2024. Advancing air quality prediction models in urban India: A deep learning approach integrating DCNN and LSTM architectures for AQI time-series classification. Model Earth Syst Environ. 10(2):2935-2955.
7. Samal KKR, Panda AK, Babu KS, Das SK. 2021. An improved pollution forecasting model with meteorological impact using multiple imputation and fine-tuning approach. Sustain Cities Soc. 70:102923.
8. Kalantari E, Gholami H, Malakooti H, Nafarzadegan AR, Moosavi V. 2024. Machine learning for air quality index (AQI) forecasting: Shallow learning or deep learning? Environ Sci Pollut Res. 31(54):62962-62982.
9. Bhatti UA, Tang H, Wu G, Marjan S, Hussain A. 2023. Deep learning with graph convolutional networks: An overview and latest applications in computational intelligence. Int J Intell Syst. 2023:8342104.
10. Han H, Liu Z, Barrios M, Li J, Zeng Z, Sarhan N, *et al*. 2024. Time series forecasting model for non-stationary series pattern extraction using deep learning and GARCH modeling. J Cloud Comput. 13(1):2.
11. Biscaya S, Elkadi H, Pramanik M, Linn KN. 2024. BREATHE-Cities: Bolstering resilience and environmental air-quality through transformative healthy emission transport in cities. Bath (UK): University of Bath; 91 p.
12. Zhao Y, Sun H, Tang J, Li Y, Sun Z, Tao Z, *et al*. 2023. Environmental risk assessment of the Harbin section of the Songhua River Basin based on multisource data fusion. Water. 15(24):4293.
13. Zhang S, Cao J, Gao Y, Sun F, Yang Y. 2025. A deep learning algorithm for multisource data fusion to predict effluent quality of wastewater treatment plant. Toxics. 13(5):349.
14. Cai J, Liu T, Wang T, Feng H, Fang K, Bashir AK, *et al*. 2024. Multisource fusion enhanced power-efficient sustainable computing for air quality monitoring. IEEE Internet Things J. 11(24):39041-39055.
15. Jiang Y, Li C, Song H, Wang W. 2022. Deep learning model based on urban multisource data for predicting heavy metals (Cu, Zn, Ni, Cr) in industrial sewer networks. J Hazard Mater. 432:128732.
16. Wang S, Wu M, Wei X, Song X, Wang Q, Jiang Y, *et al*. 2025. An advanced multisource data fusion method utilizing deep learning techniques for fire detection. Eng Appl Artif Intell. 142:109902.
17. Chen L, Long H, Xu J, Wu B, Zhou H, Tang X, *et al*. 2023. Deep citywide multisource data fusion-based air quality estimation. IEEE Trans Cybern. 54(1):111-122.
18. Zhang Z, Wang X, Li Y, Liu Y, Xu Y, Li J, *et al*. 2024. River ecosystem health assessment in the Qinghai-Tibet Plateau: A novel hybrid method based on artificial intelligence and multisource data fusion. Expert Syst Appl. 251:124078.

19. Wang B, Hua L, Mei H, Kang Y, Zhao N. 2023. Monitoring marine pollution for carbon neutrality through a deep learning method with multisource data fusion. Front Ecol Evol. 11:1257542.